Aging Cell (2009) **8,** pp654–665 Doi: 10.1111/j.1474-9726.2009.00519.x

Dysfunction of the unfolded protein response increases neurodegeneration in aged rat hippocampus following proteasome inhibition

María Paz Gavilán,[1,2] Cristina Pintado,[1,3,4] Elena Gavilán,[1,2] Sebastián Jiménez,[1,3,4] Rosa M. Ríos,[2] Javier Vitorica,[1,3,4] Angélica Castaño[1,3,4] and Diego Ruano[1,3,4]

[1]Departamento de Bioquímica, Bromatología, Toxicología y Medicina Legal, Facultad de Farmacia, Universidad de Sevilla, Sevilla, Spain
[2]Departamento de Señalización Celular, Centro Andaluz de Biología Molecular y Medicina Regenerativa (CABIMER), Avda, Americo Vespucio s/n, 41092-Sevilla, Spain
[3]Instituto de Biomedicina de Sevilla (IBiS)-Hospital Universitario Virgen del Rocío/CSIC/Universidad de Sevilla, Sevilla, Spain
[4]Centro de Investigación Biomédica en Red sobre Enfermedades Neurodegenerativas (CIBERNED) 41013-Sevilla, Spain

Summary

Dysfunctions of the ubiquitin proteasome system (UPS) have been proposed to be involved in the aetiology and/or progression of several age-related neurodegenerative disorders. However, the mechanisms linking proteasome dysfunction to cell degeneration are poorly understood. We examined in young and aged rat hippocampus the activation of the unfolded protein response (UPR) under cellular stress induced by proteasome inhibition. Lactacystin injection blocked proteasome activity in young and aged animals in a similar extent and increased the amount of ubiquitinated proteins. Young animals activated the three UPR arms, IRE1α, ATF6α and PERK, whereas aged rats failed to induce the IRE1α and ATF6α pathways. In consequence, aged animals did not induce the expression of pro-survival factors (chaperones, Bcl-XL and Bcl-2), displayed a more sustained expression of pro-apoptotic markers (CHOP, Bax, Bak and JKN), an increased caspase-3 processing. At the cellular level, proteasome inhibition induced neuronal damage in young and aged animals as assayed using Fluorojade-B staining. However, degenerating neurons were evident as soon as 24 h postinjection in aged rats, but it was delayed up to 3 days in young animals. Our findings show evidence supporting age-related dysfunctions in the UPR activation as a potential mechanism linking protein accumulation to cell degeneration. An imbalance between pro-survival and pro-apoptotic proteins, because of noncanonical activation of the UPR in aged rats, would increase the susceptibility to cell degeneration. These findings add a new molecular vision that might be relevant in the aetiology of several age-related neurodegenerative disorders.

Key words: aging; Alzheimer; apoptosis; ER-stress; neuroinflammation; UPR.

Introduction

The proteasome is responsible for the majority of cellular proteolysis by degrading multiple substrates that are important for maintaining cellular viability (Pines and Lindon, 2005). In consequence, proteasome dysfunctions could produce severe disturbances in cellular homeostasis, which should be restored by the activation of specific cellular responses to assure cell viability. Impairments in proteasome activity have been observed in Alzheimer's disease (AD) (Keller *et al.*, 2000a; Lopez-Salon *et al.*, 2000; Keck *et al.*, 2003) and in normal aging (Keller *et al.*, 2000b; Gavilán *et al.*, 2006). Indeed, paired helical filament-tau from brains of patients with AD (Keck *et al.*, 2003) or oligomeric forms of the Aβ peptide purified from a transgenic mouse model of AD (Tseng *et al.*, 2008) inhibited proteasome activity. In the same way, we have previously shown that proteasome inhibition in rat hippocampus alters the endoplasmic reticulum (ER) homeostasis, producing ER stress and inducing the UPR (Gavilán *et al.*, 2006). This cellular response is mediated by the activation of three signalling pathways (IRE1α, ATF6α and PERK) and is characterized by the: (i) up-regulation of genes coding for different molecular chaperones; (ii) attenuation of protein translation and (iii) proteasomal degradation of misfolded proteins (Mori, 2000; Kaufman, 2002). However, whether ER stress persists, cellular apoptosis is activated (Szegezdi *et al.*, 2006).

In this line, ER stress has been proposed to mediate cellular degeneration in a number of human diseases including AD (Kaufman, 2002; Lindholm *et al.*, 2006; Yoshida, 2007). Similarly, disturbed activation of ER stress transducers has been described in cell culture from mice model of familial AD-linked Presenilin-1 mutations (Katayama *et al.*, 2001), but data from sporadic AD cases are still lacking. Nevertheless, the mechanisms linking proteasome dysfunction, ER stress and cell degeneration are currently poorly understood.

Taking into account that aging is the most relevant risk factor to develop AD and that animal models of the sporadic variant are lacking, it is essential to gain insight into how cells respond

Correspondence
Dr Diego Ruano, Departamento de Bioquímica y Biología Molecular, Facultad de Farmacia, C/ Profesor García González nº 2, 41012-Sevilla, Spain. Tel.: +34 95455 6220; fax: +34 95423 3765; e-mail: ruano@us.es

Accepted for publication *14 August 2009*

Aging Cell

to cellular stress induced by protein accumulation in normal aged brain, to better understand the pathophysiological states. Therefore, we have evaluated at the molecular and cellular levels in young and aged animals, the role of ER stress in mediating cell degeneration, occasioned by protein accumulation induced by proteasome inhibition. We have analysed the UPR activation and found that aged animals did not induce efficiently it. The inefficient UPR activation sensitized aged cells to ER stress degeneration. Our data support that age-related dysfunctions in UPR activation may represent a link between protein accumulation and cell degeneration in aged animals. Present data could contribute to understand the mechanisms underlying the higher probability to develop AD during aging.

Results

UPR activation induced by lactacystin injection is defective in aged rat hippocampus

To evaluate the UPR activation induced by proteasome inhibition and the potential age-related modifications in young and aged rat hippocampus, we performed a time-course analysis of the three cellular pathways involved in the activation of the UPR (IRE1α, ATF6α and PERK), following lactacystin injection.

As shown (Fig. 1A), lactacystin injection blocked chymotrypsin activity in a similar extent in young and aged animals, producing the accumulation of ubiquitinated proteins (Fig. 1B) that induced ER stress (Gavilán *et al.*, 2006).

IRE1α pathway

IRE1α activation gives rise to an unconventional splicing of the XBP1 mRNA through its C-terminal endonuclease domain (González *et al.*, 1999; Calfon *et al.*, 2002), producing the spliced form of XBP1 mRNA (sXBP1). This spliced mRNA is then translated into a transcription factor that moves to the nucleus activating the IRE1α pathway. As shown in Fig. 2A, lactacystin injection significantly up-regulated (*$P < 0.05$) the mRNA expression of the XBP1 gene in young but not in aged animals. In the same way, the amount of sXBP1 mRNA significantly increased from 6 to 14 h postinjection, only in young animals (Fig. 2B). In consequence, young animals significantly increased the amount of sXBP1 mRNA with respect to treated aged rats (#$P < 0.05$). The nuclear amount of this transcription factor was also evaluated, using proteins from the nuclear fraction of the same young and aged animals. As shown in Fig. 2C,D, the amount of processed (active) pXBP1 protein (Mr of 50 kDa) remained unchanged in young animals from 6 to 14 h following lactacystin injection, with respect to young control animals. However, in aged animals the amount of pXBP1 protein significantly decreased at 6 and 14 h postinjection (*$P < 0.05$), with respect to aged controls, and also with respect to young treated animals at 14 h postinjection (#$P < 0.05$). As also shown in Fig. 2C, samples from aged rats showed a protein of Mr 30 kDa (at 6 h postinjection) that, probably corresponded to the unprocessed XBP1 (uXBP1) protein (Yoshida *et al.*, 2006, 2009). This protein, which is rapidly degraded by the proteasome (Tirosh *et al.*, 2006), is hardly detected by immunoblotting (Yoshida *et al.*, 2006) and acts as a negative regulator of the UPR activation (Lee *et al.*, 2003; Yoshida *et al.*, 2006; Tirosh *et al.*, 2006; Yoshida *et al.*, 2009).

The IRE1α pathway is also linked to the c-Jun N-terminal kinase (JNK) pathway through formation of an IRE1α–TRAF2–ASK1 complex (Urano *et al.*, 2000; Nishitoh *et al.*, 2002). So, we also analysed the activation of this pathway by western blots

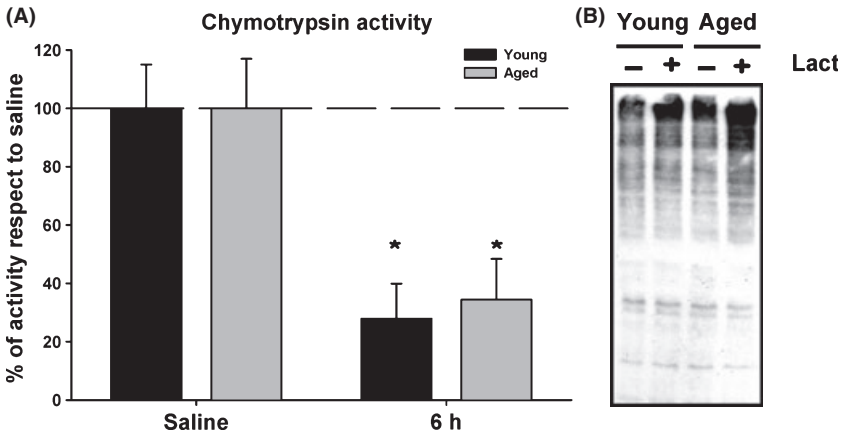

Fig. 1 Lactacystin injection blocks proteasome activity and induces protein accumulation in both young and aged hippocampus. (A) Proteasome activity was assessed by quantification after the hydrolysis of a fluorogenic substrate specific for the chymotrypsin-like activity (LLVY-AMC), in samples from young and aged lactacystin-treated rats (6 h postinjection). Data are presented as the mean ± SD relative to the activity of saline-injected animals. Data were obtained from triplicate assays. A similar inhibition was observed in young and aged treated rats. (B) Ubiquitinated protein, predominantly those of higher molecular weight, accumulated in young and aged rat hippocampus following lactacystin injection. Shown is a representative western blot corresponding to saline-injected animals (young and aged), and lactacystin-injected rats (6 h postinjection). As previously described (Gavilán *et al.*, 2006), aged rats showed higher amount of ubiquitinated proteins than young animals. *$P < 0.05$, significant differences compared to saline animals.

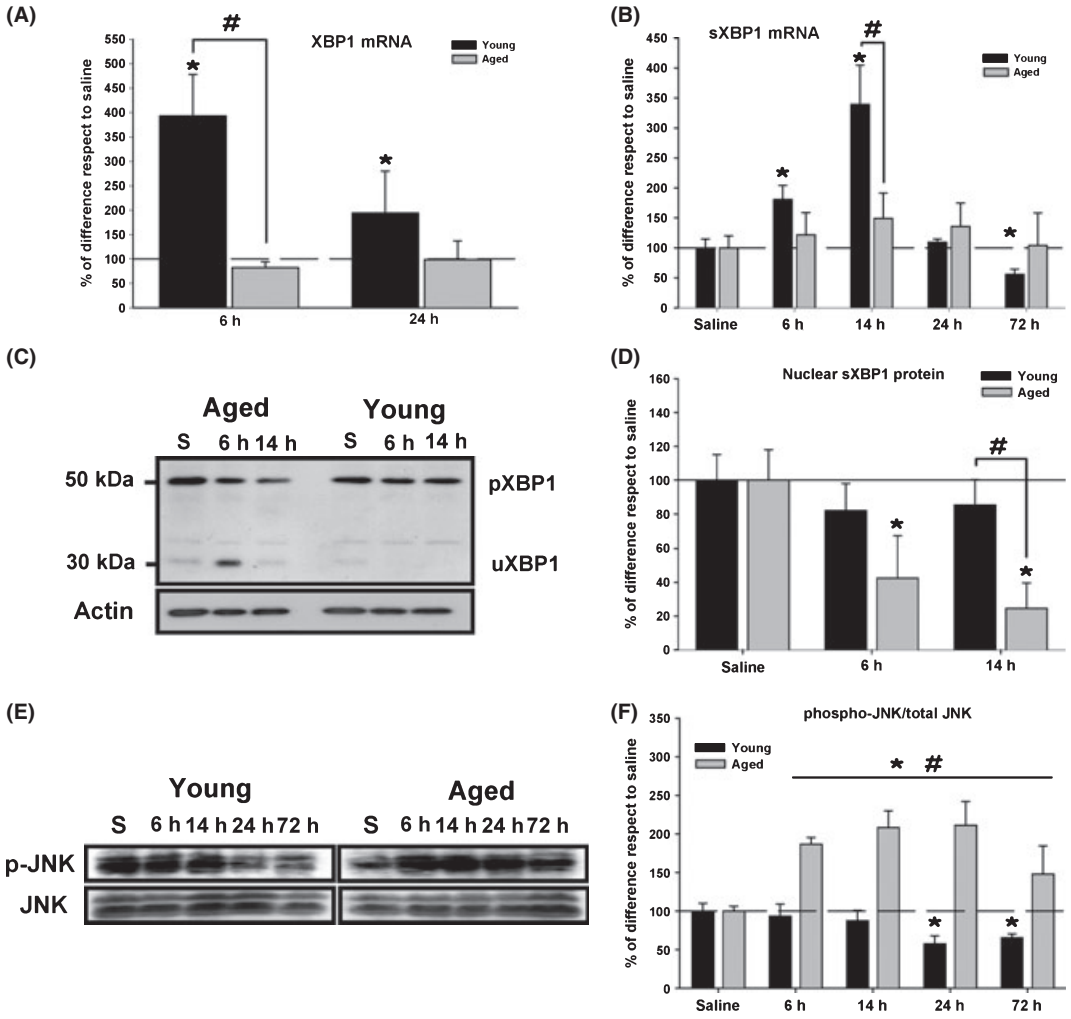

Fig. 2 Molecular markers of the IRE1α pathway expressed in young and aged rat hippocampus following lactacystin injection. mRNA expression of total XBP1 (A) and spliced XBP1 (B), analysed by RT-real time PCR, was up-regulated in young (n = 4/time point), but not in aged rat hippocampus (n = 4/time point) following lactacystin injection. (C) Western blot of the XBP1 protein in the nuclear fraction of the same young and aged rats. The band of Mr 50 kDa, (pXBP1) corresponded to the processed active transcription factor. The band of Mr 30 kDa corresponded to the un-processed (uXBP1) protein and was exclusively observed in aged animals from 6 to 14 h postlactacystin injection. (D) Optical density analysis of western blots. Data are presented as mean ± SD of four independent experiments, each one including one young and one aged animal at different times postlactacystin injection. (E) Western blot analysis of the phospho-JNK (upper panel) and total-JNK (lower panel) expressed in young and aged rats following lactacystin injection. (F) Optical density analysis of western blots. Data are presented as mean ± SD of four independent experiments, each one including one young and one aged animal at different times postlactacysitn injection. *P < 0.05, significant differences compared to saline animals. #P < 0.05, significant differences between young and aged animals.

using anti-phospho and total JNK antibodies, in young and aged rats following proteasome inhibition. As shown in Fig. 2E, in young animals the amount of phospho-JNK proteins remained similar to saline-injected animals up to 14 h postlactacystin injection, decreasing then from 24 to 72 h. By contrast, in aged rats lactacystin injection produced a rapid and sustained phosphorylation of the JNK proteins (from 6 to 72 h). In consequence, the phospho-JNK/total JNK ratio was significantly increased with respect to saline-injected aged animals, and also with respect to young animals (*, #P < 0.05) at all times postinjection (Fig. 2F). These results suggest that proapoptotic branch of the IRE1α pathway is active in aged animals. However activation of JNK pathway may be due to other ER stress independent stimuli (see Discussion).

ATF6α pathway

The mRNA expression of the ATF6α protein was analysed using RT-real time PCR in the same group of young and aged animals. ATF6α mRNA expression was significantly up-regulated (*P < 0.05), with respect to saline-injected animals, in young but no in aged rats (Fig. 3A), becoming significantly higher (#P < 0.05) at 24 h postinjection in young with respect to aged treated animals. Under ER stress conditions, full-length ATF6α protein (90 kDa) is sequentially cleaved in the Golgi apparatus using S1P and S2P proteases, to yield $pATF6_{50}$ (50 kDa) that migrates into the nucleus. As shown in Fig. 3B,C, in our model the amount of $pATF6_{50}$ protein significantly decreased (*P < 0.05) in the nuclear fraction of both young and aged rats early as 6 h postinjection. However, at 14 h young animals

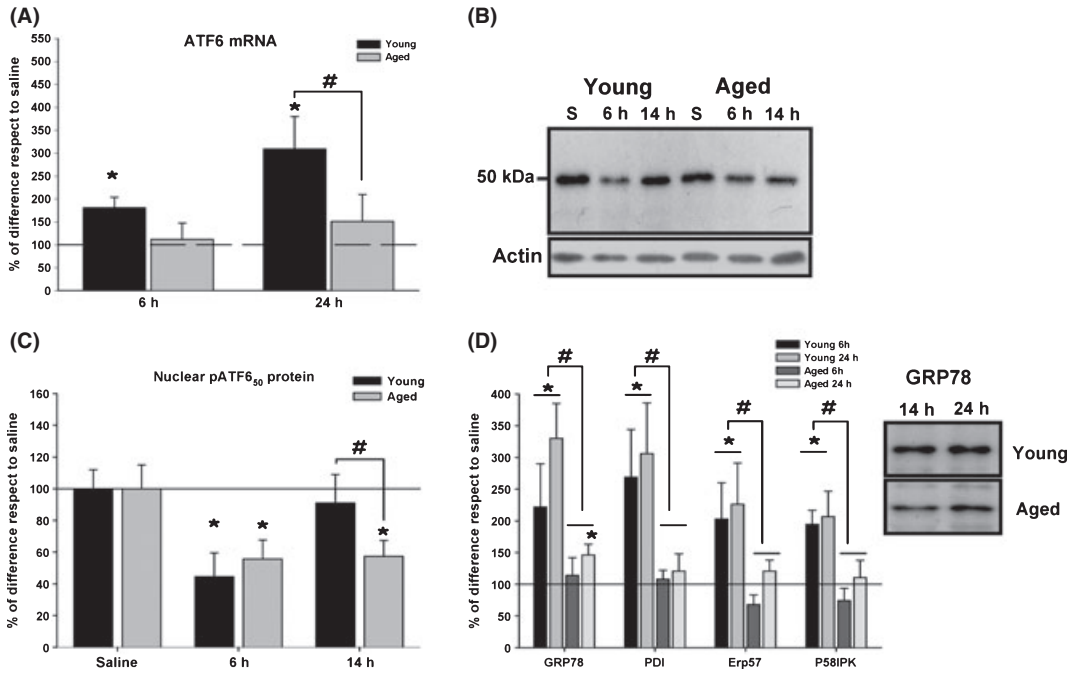

Fig. 3 Molecular markers of the ATF6α pathway expressed in young and aged rat hippocampus following lactacystin injection. (A) mRNA expression of ATF6α was up-regulated in young but not in aged rat hippocampus following lactacystin injection. (B) Representative western blot of the active transcription factor pATF6$_{50}$ in the nuclear fraction of young and aged rats. (C) Optical density from western blots. Data are presented as the mean ± SD of four independent experiments, each one including one young and one aged animal at different times postlactacystin injection. (D) mRNA expression of the ER chaperones GRP78, PDI, Erp57 and P58IPK following lactacystin injection in young and aged rats. All the mRNAs analysed were significantly up-regulated in young animals in a time-dependent manner. In aged rats, only the GRP78 mRNA was significantly up-regulated at 24 h postinjection. In the insert is shown a representative western blot of the GRP78 protein expressed in young and aged animals at 14 and 24 h postinjection (samples for four animals were pooled per time point; see also Gavilán *et al.*, 2006). *$P < 0.05$, significant differences compared to young or aged saline animals. #$P < 0.05$, significant differences between young and aged animals.

recovered the basal level whereas in aged rats remained significantly lower (*$P < 0.05$). This transcription factor mainly regulates the expression of proteins involved in the ER protein folding, such as molecular chaperones (Yoshida *et al.*, 2000; Ma *et al.*, 2002; Yoshida, 2007). So, we analysed the mRNA expression of several ER chaperones. As shown in Fig. 3D, the mRNA expression of GRP78, PDI, Erp57 and P58IPK was significantly up-regulated (*$P < 0.05$) in young animals from 6 to 24 h postinjection with respect to young control animals. By contrast, in aged rats only the mRNA expression of GRP78 was moderately but significantly up-regulated (*$P < 0.05$) just at 24 h postinjection (Fig. 3D). As a result the mRNAs of ER chaperones were significantly up-regulated (#$P < 0.05$) in young with respect to aged animals. In the same way, protein expression of GRP78 remained unchanged in aged but not in young animals (insert in Fig. 3D, see also Gavilán *et al.*, 2006). This effect appeared to be more specific for the ER chaperones because the mRNA expression of Hsp70 (a cytoplasmic chaperone) was significantly up-regulated in both, young and aged rats from 14 to 24 h following lactacystin injection (data not shown).

PERK pathway

PERK activation produces the phosphorylation of the α subunit of the eukaryotic translation initiation factor-2 (eIF2α) thus, attenuating global protein synthesis (Novoa *et al.*, 2001). So, we analysed in young and aged treated animals the eIF2α phosphorylation level as a marker of the PERK pathway activation. As shown in Fig. 4A,B, lactacystin injection significantly increased (*$P < 0.05$) the phospho-eIF2α/total eIF2α ratio, in young and aged rats, as soon as 6 h postinjection. In young animals, the increase in the phospho-eIF2α/total eIF2α ratio was followed by a significant decrease at 14 h (*$P < 0.05$), to finally reach the basal level from 24 to 72 h. On the contrary, aged rats returned to basal level from 14 to 72 h, but in a gradual manner. Importantly, the abrupt decrease in p-eIF2α, observed in young animals 14 h after injection was totally lost in aged rats. This age-related difference could be consequence of the lower mRNA expression of the gene coding for the GADD34 protein in aged respect to young animals (Fig. 4C). GADD34 is an UPR-induced gene that encodes a β-subunit of the protein phosphatase 1 involved in eIF2α dephosphorylation (Novoa *et al.*, 2001). mRNA up-regulation of GADD34 was sustained from 6 to 24 h postinjection in young and aged animals but with different intensity (in average, ten and fourfolds of increase respect to saline animals for young and aged rats respectively).

Phosphorylation of eIF2α leads to a transient suppression of general translation, but increases translation of the mRNA for ATF4 as a consequence of a ribosome-scanning mechanism and two short upstream open reading frames in the ATF4 mRNA (Lu *et al.*, 2004; Vattem & Wek, 2004). As shown in Fig. 4D, in

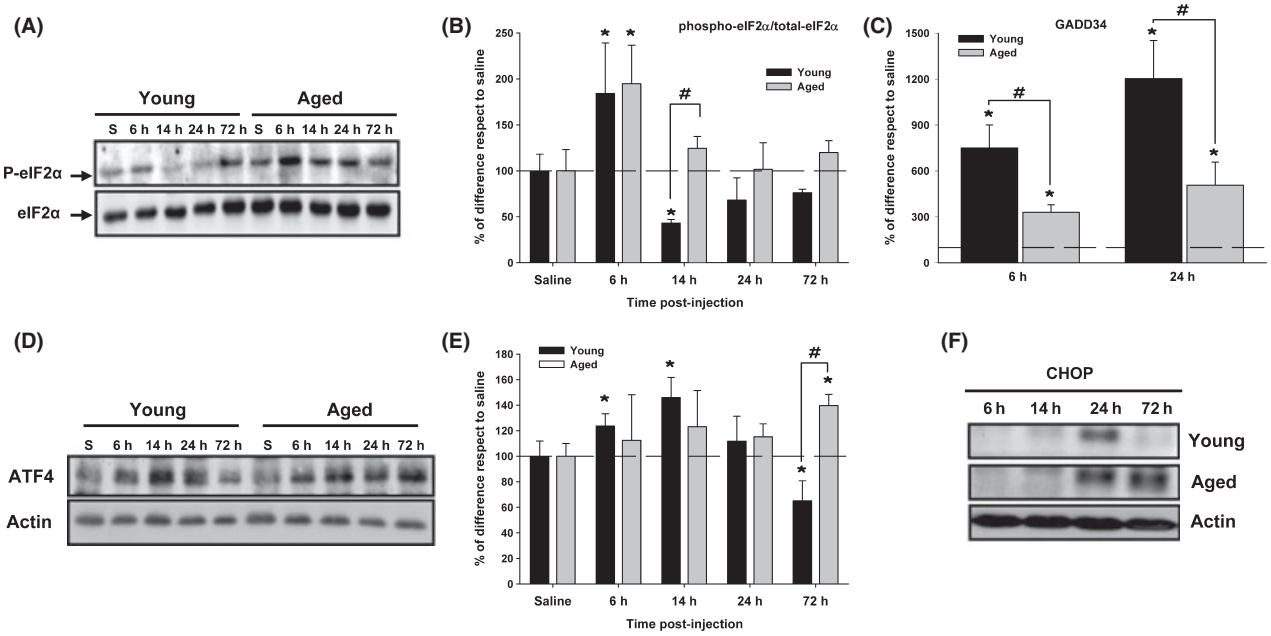

Fig. 4 Molecular markers of the PERK pathway expressed in young and aged rat hippocampus following lactacystin injection. (A) Representative western blot of the phospho-eIF2α (P-eIF2α) and total eIF2α proteins expressed in the cytosolic fraction of young and aged rat hippocampus following lactacystin injection. Membranes were first incubated with a specific antibody against P-eIF2α, and then incubated with a second specific antibody against total eIF2α. (B) Optical density analysis of western blots. Shown is the P-eIF2α/eIF2α ratio. Data are represented as mean ± SD of four independent experiments, each one including one young and one aged animal at different times postlactacystin injection. The P-eIF2α/eIF2α ratio was significantly increased in young and aged animals at 6 h postinjection and rapidly decreased in young but not in aged rats at 14 h postinjection. (C) mRNA expression of GADD34 was significantly up-regulated in young an aged animals following lactacystin injection. (D) Representative western blot corresponding to the transcription factor ATF4 in the nuclear fraction of young and aged animals following lactacystin injection. (E) Optical density analysis of western blots. Data are presented as mean ± SD of four independent experiments, each one including one young and one aged animal at different times postlactacystin injection. ATF4 protein was significantly increased in the nuclear fraction of young animals from 6 to 14 h and significantly decreased at 72 h. Aged rats also tended to increase the nuclear content of ATF4 during the first 24 h, however a significant increase was noted at 72 h. (F) Representative western blot corresponding to the transcription factor CHOP. The pro-apoptotic factor CHOP was exclusively observed in the nuclear fraction at 24 h after lactacystin injection in young rats. In aged rats, CHOP expression was also first detected at 24 h but was sustained up to 72 h. The experiment was done twice with similar results. Beta-actin corresponded to aged samples. Not differences with respect to young β-actin samples were observed (not shown). *$P < 0.05$, significant differences compared to saline animals. #$P < 0.05$, significant differences between young and aged animals.

contrast to the transcription factors pXBP1 and pATF6(50), ATF4 protein was significantly increased (*$P < 0.05$) in the nuclear fraction of young animals from 6 to 14 h postinjection. In aged rats, ATF4 protein also tended to increase during the first 24 h, reaching a significant increase, at 3 days postinjection, with respect to both, saline-injected animals and young rats (#,*$P < 0.05$). Interestingly, the increased translation of ATF4 leads to induction of ATF4-responsive genes involved in the ER stress response, such as the pro-apoptotic transcription factor CHOP. As CHOP needs to be translocated and accumulated into the nucleus to induce apoptosis (Zinszner *et al.*, 1998), we next analysed the expression of CHOP protein in nuclear fractions of young and aged treated rats. As shown in Fig. 4F, CHOP protein was clearly detected at 24 h postinjection in the nuclear fraction of both young and aged animals. However, at 72 h postinjection the nuclear content of CHOP was imperceptible, in young, but remained high in aged animals.

Altogether, these results strongly support that lactacystin-induced ER stress produced a canonical UPR activation (IRE1α-XBP1, ATF6α and PERK-eIF2α signalling pathways) in young animals, whereas in aged rats the IRE1α-XBP1 and ATF6α pathways were not efficiently activated.

The pro-apoptotic proteins Bax a Bak and the pro-survival proteins Bcl-XL and Bcl-2 are differentially expressed in young and aged lactacystin-treated rats

The UPR includes pro-survival and pro-apoptotic pathways (Rutkowski & Kaufman, 2007; Yoshida, 2007). As aged rats did not efficiently induce the UPR, we examined whether this age-related dysfunction affected the balance between UPR-induced pro-apoptotic and pro-survival proteins. For that, we analysed the expression of two pro-apoptotic and two pro-survival proteins of the Bcl-2 family related to ER stress (Rudner *et al.*, 2002; Thomenius *et al.*, 2003; Hetz *et al.*, 2006). As shown in Fig. 5A,B, the expression profile of pro-apoptotic proteins Bax an Bak in young rats was the opposite of that observed for aged animals. Whereas the expression of these two pro-apoptotic proteins was significantly decreased in young animals (*$P < 0.05$) they were significantly increased in aged animals (#,*$P < 0.05$). By contrast, the expression of the pro-survival proteins Bcl-2 (*$P < 0.05$) and Bcl-XL (#,*$P < 0.05$) was significantly increased in young rats, but decreased in aged animals (Fig. 5C,D). Thus, these findings demonstrate the existence of an age-related imbalance between anti- and pro-apoptotic

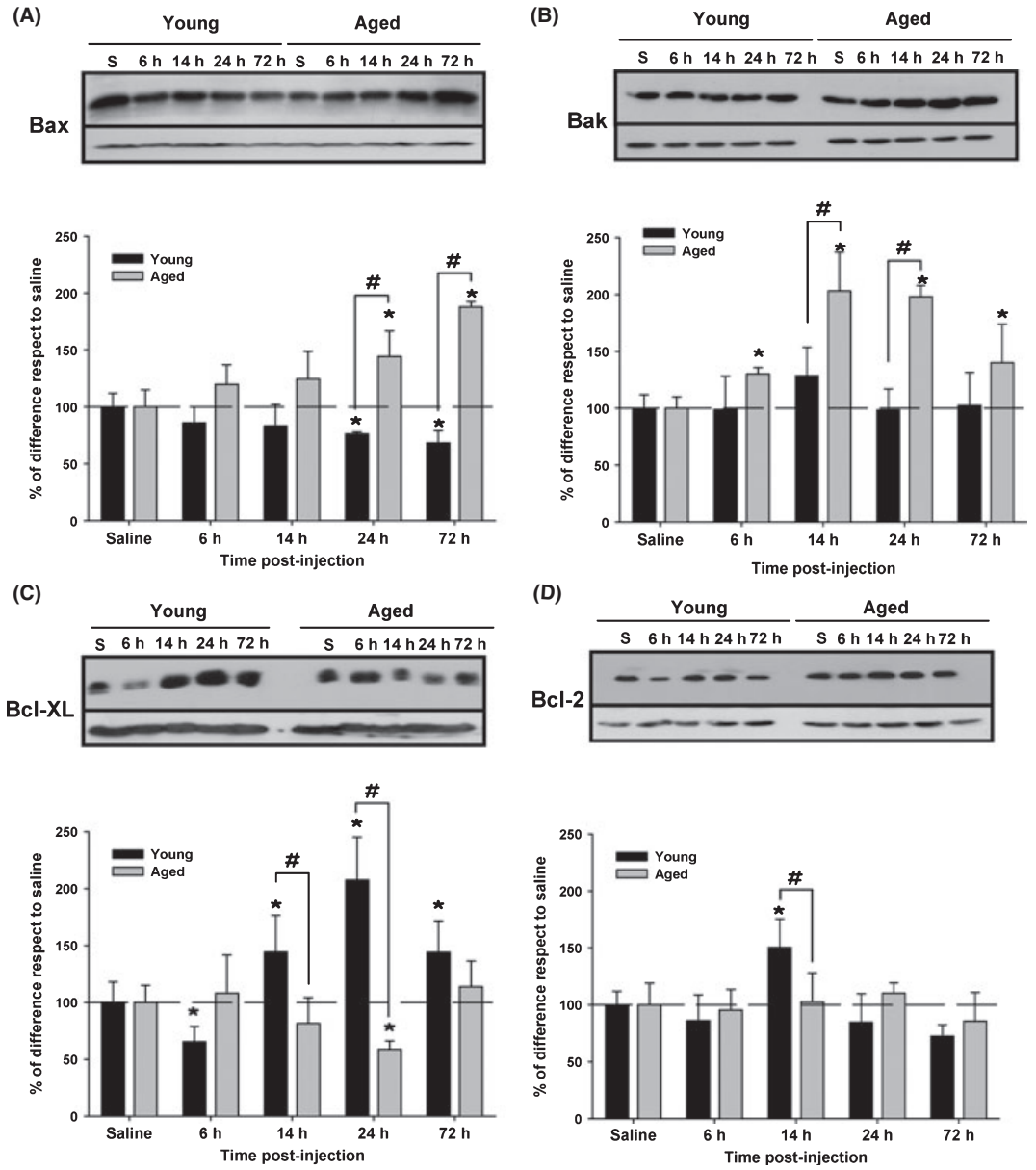

Fig. 5 Pro-apoptotic and pro-survival proteins expressed in young and aged rat hippocampus following lactacystin injection. Representative western-blots and densitometric analysis of pro-apoptotic proteins Bax (A) and Bak (B) and the anti-apoptotic proteins Bcl-XL (C) and Bcl-2 (D). In aged rats, the pro-apoptotic proteins Bax and Bak were significantly increased from 24 to 72 h, and from 6 to 72 h respectively. Young animals did not modify or even decreased the expression of these two pro-apoptotic proteins. On the contrary, young animals displayed and increase in the expression of the pro-survival proteins Bcl-XL (from 14 to 72 h pos-lactacystin injection), and Bcl-2 (14 h), whereas aged rats did not modify, or even decreased, the expression of these two pro-survival proteins. Interestingly, Bcl-XL was significantly decreased at 6 h postinjection. $*P < 0.05$, significant differences compared to saline animals. $\#P < 0.05$, significant differences between young and aged animals.

proteins, following lactacystin injection, resulting in a prolonged expression of pro-apoptotic markers in aged rat hippocampus.

Lactacystin injection increased neurodegeneration and caspase-3 processing in aged with respect to young rats

We also analysed at the cellular level whether lactacystin injection induced cellular degeneration. Coronal sections of a new population of young ($n = 6$) and aged ($n = 6$) lactacystin-treated animals (24 h and 3 days postinjection) was stained with Fluorojade-B. As shown in Fig. 6, saline-injected animals did not show Fluorojade-B stained cells (A1-B1 and A2-B2, for young and aged rats respectively). At 24 h postinjection, young animals showed a few Fluorojade-B positive cells located near the trace of injection (CA1 region). However, aged rats showed a qualitative increase in the number and intensity of Fluorojade-B positive cells. Positive neurons were not exclusively located near the

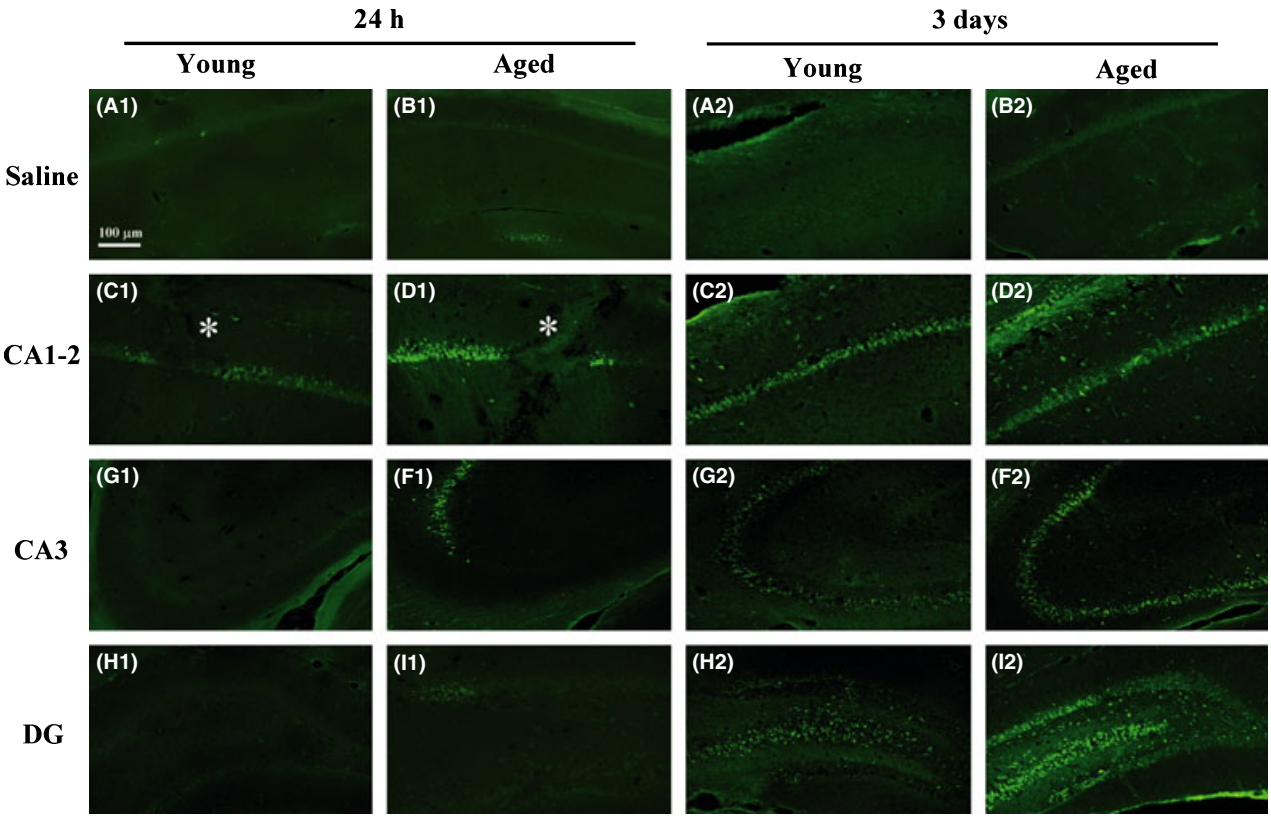

Fig. 6 Higher susceptibility to neurodegeneration in aged rats following lactacystin injection. Cellular degeneration was analysed by Fluorojade-B staining in brain sections from young and aged lactacystin-treated rats. Analysis was performed at 24 h (A1–I1) and 3 days postinjection (A2–I2). (C1, G1, H1) After 24 h, lactacystin injection did not induce cellular degeneration in young rat hippocampus (n = 3, 6 sections/animal) and only a moderate staining for Fluorojade-B was only observed at the injection track (CA1 region, asterisk). (D1, F1, I1) Aged animals showed Fluorojade-B positive neurons at the injection track (CA1 region, asterisk), and also in the CA3 region and granular layer of the dentate gyrus (distal from the injection site) (n = 3, 6 sections/animal). (C2, G2, H2) At 3 days postinjection, in young animals the number of Fluorojade-B positive neurons progressed from CA1 to CA3 and the hilar region of dentate gyrus. (D2, F2, I2) Aged rats displayed a similar pattern of cellular degeneration as observed for young rats, but qualitatively, a higher number and more intensity of Fluorojade-B positive neurons were observed in aged rats, predominantly in the CA3 and dentate gyrus regions.

trace of injection, but also in the pyramidal and granular layer of the CA3 and dentate gyrus respectively. Interestingly, in young rats after 3 days postinjection, the neurodegeneration spreads progressively from injection zone (CA1) to the whole hippocampal formation (CA3, dentate gyrus and hilar region) in both, young and aged animals. However, aged rats showed an evident increase in the number and intensity of Fluorojade-B positive cells, respect to young animals, mostly at the CA3 and granular layer (Fig. 6 G2-H2 and F2-I2, for young and aged rats respectively). The putative cell degeneration revealed using Fluorojade-B staining was further confirmed by cresyl violet staining. As shown in Fig. 7, aged rats showed a clear qualitative difference in the amount of cresyl violet stained neurons mostly in the CA3 region, with respect to both, aged saline-injected (compare a2 with b2) and young lactacystin-treated rats (compare b2 with b1). Currently, the reasons for this apparent higher sensitivity of the CA3 neurons to lactacystin injection remain to be analysed.

Finally, we evaluated whether higher neurodegeneration observed in lactacystin-treated aged rats was also reflected in a higher processing of the executioner caspase-3. As shown in Fig. 7B, procaspase-3 processing was strongly increased in aged with respect to young treated animals at both, 24 and 72 h, whereas in young animals a modest increase was observed just at 72 h postinjection.

Discussion

The overall aim of the present work was to identify potential mechanisms linking age-dependent neuronal vulnerability and protein accumulation. For that, we have examined the UPR activation in young and aged rat hippocampus following proteasome inhibition as a potential factor. This issue is of special relevance considering that impairments in the proteasome-mediated degradation pathway have been propose to contribute to the development of several age-related neurodegenerative disorders including AD (Keller *et al.*, 2000a; Keck *et al.*, 2003; Katayama *et al.*, 2004; Cecarini *et al.*, 2007). However, the mechanisms underlying cell degeneration caused by protein accumulation are still elusive. The most relevant finding shown in this work is the existence of age-related deficits in the UPR activation following proteasome inhibition that could

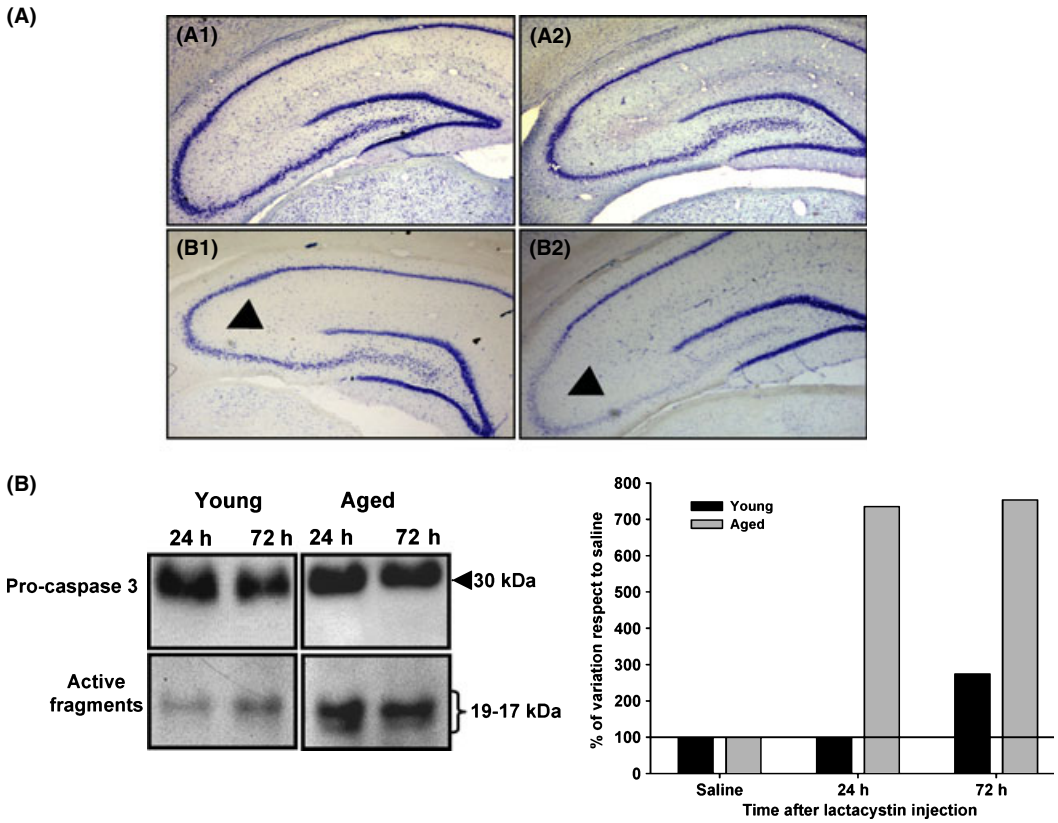

Fig. 7 Cresyl violet staining and caspase-3 processing in young and aged rat hippocampus following lactacystin injection. (A) Representative coronal sections from young: saline (a1) and 3 days postlactacystin injection (b1); and aged: saline (a2) and 3 days postlactacystin injection (b2), stained with cresyl violet. Cresyl violet positive neurons were qualitatively decreased in young and aged rats at 3 days following lactacystin injection respect to saline-injected animals. Importantly aged rats showed a more extensive loss of cresyl violet staining than young animals in the CA3 region (arrows). (B) Representative western blot analysis showing procaspase-3 (30 kDa) and the processed fragments (17–19 kDa) at 24 and 72 h postlactacystin injection in young and aged animals. Active fragments were evident in aged animals from 24 to 72 h postlactacystin injection, whereas in young animals, the processed fragments were barely detected. Both, pro-caspase and processed fragments corresponded to the same gel. To a better visualization, the portion corresponding to the processed fragments were overexposed. Shown is also the optical density analysis of western blots. Data are presented as mean of two independent experiments, each one including young and aged animals at different times postlactacystin injection (four animals pooled/time point/group).

compromise cell viability. We report novel data potentially relevant to cell apoptosis induced by ER-stress that are summarized as follows. (i) Lactacystin injection induced a canonical UPR activation in young rats, but an inefficient UPR activation in aged rats. (ii) Following lactacystin injection, young animals predominantly and early expressed pro-survival factors, whereas in aged rats were mainly induced pro-apoptotic factors. (iii) Neurodegeneration induced using lactacystin injection was earlier observed in aged animals.

UPR activation in young and aged rat hippocampus

Following lactacystin injection, young rats induced an early and simultaneous activation of the three UPR pathways. The sXBP1 and ATF6α mRNAs, in addition to the phosphorylation of eIF2α, were quickly increased. However, the protein level of these transcription factors, pXBP1 and $pATF6_{50}$, were not altered in the nuclear fractions. The reasons for this apparent discrepancy are actually unknown. One potential explanation could be attributable to the PERK-dependent protein translation attenuation occurring during UPR (Harding *et al.*, 2000, 2002; Novoa *et al.*, 2001; DeGracia *et al.*, 2002). In this line, *in vitro* experiments estimated that, 6 h after induction of ER stress, translation represent 38%, respect to baseline levels (Marciniak *et al.*, 2004). So, as we observed in this work, at the earliest phase of UPR activation the increase in the mRNA expression could produce no variation (or even decrease) at the protein level. This speculation is supported by the fact that the transcription factor ATF4, which escapes from protein translation inhibition during UPR activation (Lu *et al.*, 2004; Vattem & Wek, 2004), was the only transcription factor increased at 6 h postinjection. In any case, we are aware that comprehension of the UPR regulation is a very complex process that probably depends on the stressor stimulus and escape from the main goal of the present work.

Independently of the molecular mechanisms, our data clearly demonstrated that transcriptional activation of the UPR is occurring in young rats following lactacystin injection. We observed an evident up-regulation of the XBP1 mRNA

(preceding its processing), ATF6α mRNA, and also molecular chaperones (such as, GRP78, PDI, Erp57 and P58IPK), well-known downstream markers of the IRE1α and ATF6α pathways. However, none of these events were observed in aged lactacystin-treated rats. By contrast, the PERK-ATF4 pathway was also activated in aged rats. These findings support the notion that the ATF6α and IRE1α pathways are interactive, while the PERK pathway could be relatively independent (Yoshida *et al.*, 2001, 2009). Despite PERK-ATF4 pathway was activated in aged rats, a potential relevant data was that release of protein translation inhibition was more pronounced in young than in aged animals (Fig. 4B, 14 and 24 h). This fact suggests that the more persistent translation arrest that takes place in aged could be detrimental to cell viability (see DeGracia *et al.*, 2002 for a detailed review).

In this sense, the UPR activation observed in young rats was concomitant with an early predominant expression of prosurvival proteins, low caspase-3 processing and moderate hippocampal neurodegeneration. Indeed, degenerating neurons were evident only at 3 days postlactacystin injection, and in a lower extension than in aged rats. Particularly, from 24 to 72 h young animals displayed a low activation of JNK pathway, expressed low levels of Bax and Bak proteins, and transitorily expressed the UPR related pro-apoptotic factor CHOP in the nuclear fraction. On the other hand, chaperones (see also Gavilán *et al.*, 2006) and the anti-apoptotic protein Bcl-XL and Bcl-2 were up-regulated. By contrast, a different scenario was observed in aged rats. During the same postinjection period (24–72 h), aged animals showed a higher activation of the JNK pathway, higher levels of pro-apoptotic proteins Bax and Bak and a sustained expression of the pro-apoptotic factor CHOP in the nuclear fraction. Chaperones (see also Gavilán *et al.*, 2006) and the anti-apoptotic proteins were decreased or not modified. Accordingly, aged rats displayed higher caspase-3 processing, and an earlier (24 h) and higher hippocampal neurodegeneration. A similar activation of JNK pathway and high CHOP expression has been previously observed in old, with respect to young hepatocytes, under ER stress induced using two different stressors: thapsigargin and tunicamycin (Nikki & Holbrook, 2004). We are aware that activation of the JNK pathway it is not exclusively linked to IRE1α activation, but also to other signalling pathways such as initiated by Fas–FasL interaction, or TNF receptors activation, which cannot be discarded to be activated in this model.

Finally, at the present, the molecular mechanisms underlying the UPR dysfunction in aged animals are unknown. Based on our findings, we can propose that uXBP1 protein, observed exclusively in aged rats, might be acting as a dominant-negative inhibitor of pXBP1 (IRE1α pathway) and $pATF6_{50}$ (ATF6α pathway). As previously reported (Yoshida *et al.*, 2006, 2009), uXBP1 can move between the nucleus and the cytoplasm (because of the presence of a nuclear exclusion signal in the C-terminal region of uXBP1; absent in pXBP1). This uXBP1 protein attenuates the UPR activation by association with pXBP1 (Yoshida *et al.*, 2006) and $pATF6_{50}$, but not with ATF4 (Yoshida *et al.*, 2009), sequestering them from the nucleus and increasing proteasomal-dependent degradation of these complexes (Tirosh *et al.*, 2006). Importantly, overexpression of uXBP1 protein prevents an effective UPR activation and favours apoptosis in tumoral cells in response to proteasome inhibition (Lee *et al.*, 2003). Also, survival of tumoral cells seems to be related with the sXBP1/uXBP1 mRNA ratio (Davies *et al.*, 2008). In consequence, understanding the physiological causes of uXBP1 accumulation in aged cells may have a potential interest at the therapeutic level. However, we cannot discard other currently unknown mechanisms that could account for the inefficient UPR activation in aged animals.

Taken together, these data strongly suggest that an inefficient UPR activation could be a molecular link between cellular degeneration and protein accumulation due to proteasome dysfunction, which could contribute to explain why aging constitutes the major risk factor to develop degenerative diseases. Moreover, present work adds new data supporting that UPR dysfunction seems to play a role in determining cell viability under different stress conditions in aging (Naidoo *et al.*, 2008), making it attractive as therapeutic target. Further investigation will be necessary to look for similar age-related deficits in AD for which proteasome dysfunction has been described (Keller *et al.*, 2000a; Keck *et al.*, 2003; Cecarini *et al.*, 2007; Tseng *et al.*, 2008).

Experimental procedures

Animals

Young (3–4 months, 250-350 g) and aged (24–26 months, 650-750 g) male Wistar rats were provided by the animal care facility from the University of Seville. Animals were housed in either static or ventilated microisolator cages on bedding. Bedding, cages and drinking bottles were always autoclaved. Water supply was sterilized and commercial food was pasteurized. Periodically, samples of animals were subjected to complete serological, microbiological and endo- and ecto-parasitic evaluation. All animal experiments were carried out in accordance with the Guidelines of the European Union Council (86/609/EU), following the Spanish regulations (BOE 252/34367-91, 2005) for the use of laboratory animals and approved by the corresponding Scientific Committee of the University of Seville. All efforts were made to minimize the number of animals used and their suffering.

Surgery

Young male Wistar rats (n = 38) and aged male Wistar rats (n = 38) were used for surgery. Animals were anaesthetized with 400 mg kg^{-1} chloral hydrate and positioned in a stereotaxic apparatus (Kopf Instruments, Tujunga, CA, USA) to conform to the rat brain atlas (Paxinos & Watson, 1986).

Lactacystin (Sigma-Aldrich, St Louis, MO, USA) was dissolved (10 mg mL^{-1}) in a solution of sterilized phosphate-buffered saline (PBS) and 1 μL was injected into both hippocampi. Coordinates for young animals were: 4.5 mm posterior, ± 3.6 mm lateral and 3.6 mm ventral to the bregma and for aged rats were: 6.0 mm posterior, ± 4.6 mm lateral and 4.6 mm ventral to the bregma. To decide the coordinates for aged animals, four additional animals were previously injected with an inert tracer (monastral blue) at different coordinates according to Paxinos & Watson (1986). Injections were delivered over a period of 2 min each after which, the needle was left *in situ* for an additional 5 min to avoid reflux along the injection track. Animals were decapitated at 6, 14, 24 and 72 h (n = 4 per time point) after lactacystin injection and brains were quickly removed. Control animals (n = 3 per time point) were processed similarly but received in both hippocampi an intrahippocampal injection (1 μL each) of sterilized PBS (saline-injected animals). LPS injection (2.5 μg/hippocampus) was performed exactly as previously described (Gavilán *et al.*, 2009).

RNA extraction and reverse transcription

For PCR analysis, young and aged rats were previously anaesthetized as previously described and killed by decapitation. Both hippocampi (150–160 mg wet weight) were dissected, frozen in liquid N_2 and stored at –80 °C until use. Total RNA was extracted using the Tripure™ Isolation Reagent (Roche, Mannheim, Germany), according to the instructions of the manufacturer. The recovery of RNA was similar between young and aged animals (ranging from 1.2 to 1.4 μg mg^{-1} of tissue). Reverse transcription was performed using random hexamers primers exactly as previously described (Gavilán *et al.*, 2006, 2009).

Table 1 Sequences of the primer pairs used for the real-time PCR experiments

Name	Sequence (from 5′- to 3′)	Concentration (nM)	Length	% G+C
XBP1 UP	GCTTGTGATTGAGAACCAGG	300	20	50
XBP1 LO	GAGGCTTGGTGTATACATGG	300	20	50
sXBP1 UP	GCTTGTGATTGAGAACCAGG	300	20	50
sXBP1 LO	GGCCTGCACCTGCTGCGGACTC	300	22	72.7
ATF6 UP	GGACCAGGTGGTGTCAGAG	300	19	63.2
ATF6 LO	GACAGCTCTGCGCTTTGG	300	18	61.1
GRP78 UP	TCAGCCCACCGTAACAATCAAGG	300	23	43.5
GRP78 LO	CTTCCTCAGCAAACTTCTCGGCG	300	23	47.8
PDI UP	CTGCTGTTCCTGCCCAAGAGTGT	300	23	56.5
PDI LO	TGGCTCATCAGGTGGGGCTTG	300	21	61.9
ERP57 UP	AAGGGTTTTCCTACCATCTAC TTCTCA	300	27	40.7
ERP57 LO	TGGAGTTAGCTTCTTGTTGGCTG	300	23	47.8
P58IPK UP	CAGCCGCTAAAGAAGTCCTC	300	20	55
P58IPK LO	GGGTCTTCTCCGTCATCAAA	300	20	50
ACTIN UP	CGGAACCGCTCATTGCC	300	17	64.7
ACTIN LO	ACCCACACTGTGCCCATCTA	300	20	55
GADD34 UP	AGGCTGTGTTCACTCTCTTGC	300	21	52.3
GADD34 LO	GCCACATGAGCTACAGCTATCA	300	22	50

Real-time PCR

cDNAs were diluted in sterile water and used as template for the amplification by the polymerase chain reaction. Optimization and amplification of each specific gene product was performed using the ABI Prism 7000 sequence detector (Applied Biosystems, Madrid, Spain) and Sybr green™, as previously described (Gavilán *et al.*, 2006, 2009). Primers were designed using the PROBEFINDER software™ (Roche Applied Science) and are listed in Table 1. All of them flanked an intronic sequence to ensure the absence of genomic contamination. The cDNA levels of the different animals were determined using two different housekeepers (GAPDH and β-actin). The amplification of the housekeepers was done in parallel with the gene to be analysed. Similar results were obtained using both housekeepers. Thus, the results were normalized using only the β-actin expression. Threshold cycle (C_t) values were calculated using the software supplied by Applied Biosystems.

Subcellular fractionation

Young and aged rat hippocampi were homogenized in 500 μL of ice cold sucrose buffer (0.25 M sucrose, 1 mM EDTA, 10 mM Tris–HCl, pH 7.4), supplemented with protease inhibitor cocktail (Sigma). Aliquots of 150 μL were separated to RNA purification as previously described. The nuclear and the cytosolic fractions were separated by sequential centrifugation steps exactly as previously described (Gavilán *et al.*, 2009). The purity of both fractions was tested by western blot using the neuron-specific nuclear protein specific antibody, NeuN (neuronal nuclei; data not shown, see Gavilán *et al.*, 2009). Protein concentration was determined for each fraction using bovine albumin as standard (Lowry *et al.*, 1951).

Immunoblots

Immunoblots were done as previously described (Ruano *et al.*, 2000; Gavilán *et al.*, 2006, 2009). Briefly, proteins from the cellular fractions were loaded on a 12% or 14% polyacrylamide gel for electrophoresis (SDS–PAGE; Bio-Rad, Hercules, CA, USA) and then transferred to a nitrocellulose membrane (Hybond-C Extra; Amersham, Uppsala, Sweden). After blocking, membranes were incubated overnight at 4 °C, with the following primary antibodies: (i) rabbit polyclonal antibodies against: ubiquitin (Dako, Glostrup, Denmark) at a dilution of 1/1000; XBP1 (Abcam, Cambridge, UK), at 1 μg mL^{-1}; ATF6α (Santa Cruz Biotechnology, Santa Cruz, CA, USA) at a dilution of 1/1500; GRP78 (Santa Cruz Biotechnology) at a dilution of 1/2000; phospho-eIF2α; total eIF2α; phospho-JNK, JNK, Bax, Bak, Bcl-XL and Bcl-2 (Cell Signaling, Danvers, MA, USA), all of them at a dilution of 1/1000; CHOP (Santa Cruz Biotechnology) at a dilution of 1/300; caspase-3 (Stressgen, Ann Arbor, MI,

USA) at a dilution of 1/1000; (ii) mouse monoclonal antibody ATF4 (Abcam) at a dilution of 1/500 and (iii) mouse monoclonal antibody against β-actin (Sigma-Aldrich) at a dilution of 1/6000. Then, membranes were incubated with the appropriate secondary antibody (Dako), anti-rabbit, anti-goat or anti-mouse horseradish-peroxidase-conjugated, at a dilution of 1/6000 and developed using the ECL-plus detection method (Amersham).

Proteasome activity assay

Proteasome activity was determined using cytosolic fractions of young and aged saline-injected or lactacystin-treated animals (6 h postinjection). Chymotrypsin-like activity was determined using 50 μM of Suc-Leu-Leu-Val-Tyr-aminomethylcoumarin (AMC) (Sigma-Aldrich) as substrate. Assay mixtures containing 10 μg of protein, substrate and 50 mM HEPES-KOH, pH 7.5, was made up in a final volume of 100 μL. Measures were performed at 37 °C, by monitoring fluorescence emission (excitation wavelength 380 nm, emission wavelength 460 nm) on a Thermo Scientific Varioskan Flash spectral scanning multimode reader (software SCANLT, version 2.4.1). The fluorescence emission was first determined after 2 min of incubation, and taken each 15 min, during a total incubation period of 75 min. The product formation was linear during this time. Triplicate assays were performed for every young and aged rats (saline, $n = 4$/gorup and 6 h postlactacystin injection $n = 4$/goup). Activity was calculated by comparing the slopes of the curves obtained by plotting fluorescence vs. time of incubation, between saline and lactacystin-injected rats. Background activity was determined by addition of the proteasome inhibitor MG-132 (Sigma-Aldrich), at a final concentration of 10 μM.

Fluorojade-B staining

Staining with the fluorochrome Fluorojade-B was performed as a marker of damaged neurons. Young and aged animals were injected with saline ($n = 2$/group/time) or lactacystin ($n = 3$/group/time) and sacrificed at 24 and 3 days postinjection. Rats were perfused through the heart under deep anaesthesia (chloral hydrate) with 100 mL of PBS containing 10 U mL^{-1} heparin followed by 150–200 mL of 4% paraformaldehyde in phosphate buffer, pH 7.4. Brains were removed and processed as described (Gavilán *et al.*, 2007). Briefly, tissue was mounted on gelatin-coated glass plates and air-dried for 3 days. Glass plates were placed in a solution containing absolute ethanol for 3 min, followed by 70% ethanol solution for 1 min and rinsed in distilled water for 2 min. The glass plates were then placed in 0.06% solution of potassium permanganate and agitated for 15 min, before rinsing in distilled water. Finally, the glass plates were placed in a 0.0005% Fluorojade-B (Sigma-Aldrich) solution for 30 min and then rinsed in three separate distilled water baths for 1 min each. Glass plates were air-dried, placed in a solution containing xylene for 3 min and mounted for visualization.

Statistical analysis

Data were expressed as mean ± SD. All our data fit significantly to a normal distribution according to a standardized Kurtosis test. The data comparison between young and aged groups and between lactacystin-treated and saline-injected animals was done by two-tailed *t*-test. The differences between groups in the time-course experiments were measured using a one-way ANOVA followed by Tukey test. The significance was set at 95% confidence. Significant differences are referenced as $P < 0.05$ in the text (* respect to saline-injected animals or, # respect to young animals). Statistical analysis was done using the STATGRAPHICS PLUS (v 3.1) program.

Acknowledgments

The authors thank Dr Francisco Javier Díaz Corrales for helping in proteasomal activity determination, and Dr Antonia Gutierrez for technical support in histological experiments. This work was supported by (i) Fondo de Investigación Sanitaria (FIS), from Instituto de Salud Carlos III of Spain, through grants PI060781 (to DR) and PI060567 (to JV), and by (ii) Junta de Andalucía, Proyecto de Excelencia CVI-3199 (to RMR) and CVI-902. MPG and EG were recipients of a PhD and an undergraduate fellowships from Junta de Andalucía respectively. CP was recipient of a fellowship from Ministerio de Educación y Ciencia (MEC) of Spain.

Author contributions

DR designed research; MPG, CP, EG, AC and SJ performed research and analysed data; DR, JV, RMR and AC wrote the paper.

References

Calfon M, Zeng H, Urano F, Till JH, Hubbart SR, Harding HP, Clark SG, Ron D (2002) IRE1 couples endoplasmic reticulum load to secretory capacity by processing the XBP-1mRNA. *Nature* **415**, 92–96.

Cecarini V, Ding Q, Keller JN (2007) Oxidative inactivation of the proteasome in Alzheimer's disease. *Free Radic. Res.* **41**, 673–680.

Davies MPA, Barraclough DL, Stewart C, Joycel KA, Eccles RM, Barraclough R, Rudland PS, Sibson DR (2008) Expression and splicing of the unfolded protein response gene XBP-1 are significantly associated with clinical outcome of endocrine-treated breast cancer. *Int. J. Cancer* **123**, 85–88.

DeGracia DJ, Kumar R, Owen CR, Krause GS, White BC (2002) Molecular pathways of protein synthesis inhibition during brain reperfusion: implications for neuronal survival or death. *J. Cereb. Blood Flow Metab.* **22**, 127–141.

Gavilán MP, Vela J, Castaño A, Ramos B, del Río JC, Vitorica J, Ruano D (2006) Cellular environment facilitates protein accumulation in aged rat hippocampus. *Neurobiol. Aging* **27**, 973–982.

Gavilán MP, Revilla E, Pintado C, Castaño A, Vizuete ML, Moreno-González I, Baglietto-Vargas D, Sánchez-Varo R, Vitorica J, Gutiérrez A, Ruano D (2007) Molecular and cellular characterization of the age-related neuroinflammatory processes occurring in normal rat

hippocampus: potential relation with the loss of somatostatin GAB-Aergic neurons. *J. Neurochem.* **103**, 984–996.

Gavilán MP, Castaño A, Torres M, Revilla E, Caballero C, Jiménez S, García-Martínez A, Parrado J, Vitorica J, Ruano D (2009) Age-related increase in the immunoproteasome content in rat hippocampus: molecular and functional aspects. *J. Neurochem.* **108**, 260–270.

González TN, Sidrauski C, Dorfler S, Walter P (1999) Mechanism of non-spliceosomal mRNA splicing in the unfolded protein response pathway. *EMBO J.* **18**, 3119–3132.

Harding HP, Novoa I, Zhang Y, Zeng H, Wek R, Schapira M, Ron D (2000) Regulated translation initiation controls stress-induced gene expression in mammalian cells. *Mol. Cell* **6**, 1099–1108.

Harding HP, Calfon M, Urano F, Novoa I, Ron D (2002) Transcriptional and translational control in the mammalian Unfolded Protein Response. *Annu. Rev. Cell Dev. Biol.* **18**, 575–599.

Hetz C, Bernasconi P, Fisher J, Lee AH, Bassik MC, Antonsson B, Brandt GS, Iwakoshi NN, Schinzel A, Glimcher LH, Korsmeyer SJ (2006) Proapoptotic BAX and BAK modulate the unfolded protein response by a direct interaction with IRE1alpha. *Science* **312**, 572–576.

Katayama T, Imaizumi K, Honda A, Yoneda T, Kudo T, Takeda M, Mori K, Rozmahel R, Fraser P, George-Hyslop PST, Tohyama M (2001) Disturbed activation of endoplasmic reticulum stress transducers by familial Alzheimer's disease-linked presenilin-1 mutations. *J. Biol. Chem.* **276**, 43446–43454.

Katayama T, Imaizumi K, Manabe T, Hitomi J, Kudo T, Tohyama M (2004) Induction of neuronal death by ER stress in Alzheimer's disease. *J. Chem. Neuroanat.* **28**, 67–78.

Kaufman RJ (2002) Orchestrating the unfolded protein response in health and disease. *J. Clin. Invest.* **110**, 1389–1398.

Keck S, Nitsch R, Grune T, Ullrich O (2003) Proteasome inhibition by paired helical filament-tau in brains of patients with Alzheimer's disease. *J. Neurochem.* **85**, 115–122.

Keller JN, Hanni KB, Markesbery WR (2000a) Impaired proteasome function in Alzheimer's disease. *J. Neurochem.* **75**, 436–439.

Keller JN, Hanni KB, Markesbery WR (2000b) Possible involvement of proteasome inhibition in aging: implications for oxidative stress. *Mech. Ageing Dev.* **113**, 61–70.

Lee AH, Iwakoshi NN, Anderson KC, Glimcher LH (2003) Proteasome inhibitors disrupt the unfolded protein response in myeloma cells. *PNAS* **100**, 9946–9951.

Lindholm D, Wootz H, Korhonen L (2006) ER stress and neurodegenerative diseases. *Cell Death Differ.* **13**, 385–392.

Lopez-Salon M, Morelli L, Castano EM, Soto EF, Pasquini JM (2000) Defective ubiquitination of cerebral proteins in Alzheimer's disease. *J. Neurosci. Res.* **62**, 302–310.

Lowry OH, Rosebrough NJ, Farr AL, Randall RJ (1951) Protein measurement with the Folin phenol reagent. *J. Biol. Chem.* **193**, 265–275.

Lu PD, Harding HP, Ron D (2004) Translation re-initiation at alternative open reading frames regulates gene expression in an integrated stress response. *J. Cell Biol.* **167**, 27–33.

Ma Y, Brewer JW, Diehl JA, Hendershot LM (2002) Two distinct stress signaling pathways converge upon the CHOP promoter during the mammalian unfolded protein response. *J. Mol. Biol.* **318**, 1351–1365.

Marciniak SJ, Yun CY, Oyadomari S, Novoa I, Zhang Y, Jungreis R, Nagata K, Harding HP, Ron D (2004) CHOP induces death by promoting protein synthesis and oxidation in the stressed endoplasmic reticulum. *Genes Dev.* **18**, 3066–3077.

Mori K (2000) Tripartite management of unfolded proteins in the endoplasmic reticulum. *Cell* **101**, 451–454.

Naidoo N, Ferber M, Master M, Zhu Y, Pack AI (2008) Aging impairs the unfolded protein response to sleep deprivation and leads to proapoptotic signaling. *J. Neurosci.* **28**, 6539–6548.

Nikki JL, Holbrook J (2004) Elevated gadd153/chop expression and enhanced c-Jun N-terminal protein kinase activation sensitizes aged cells to ER stress. *Exp. Gerontol.* **39**, 735–744.

Nishitoh H, Matsuzawa A, Tobiume K, Saegusa K, Takeda K, Inoue K, Hori S, Kakizuka A, Ichijo H (2002) ASK1 is essential for endoplasmic reticulum stress-induced neuronal cell death triggered by expanded polyglutamine repeats. *Genes Dev.* **16**, 1345–1355.

Novoa I, Zeng H, Harding HP, Ron D (2001) Feedback inhibition of the unfolded protein response by GADD34-mediated dephosphorylation of eIF2alpha. *J. Cell Biol.* **153**, 1011–1022.

Paxinos G, Watson C (1986) *The Rat Brain in Stereotaxic Coordinates*. San Diego, CA: Academic Press.

Pines J, Lindon C (2005) Proteolysis: anytime, any place, anywhere? *Nat. Cell Biol.* **7**, 731–735.

Ruano D, Araujo F, Revilla E, Vela J, Bergis O, Vitorica J (2000) GABA-A and alpha-amino-3-hydroxy-5-methylsoxazole-4-propionate receptors are differentially affected by aging in the rat hippocampus. *J. Biol. Chem.* **275**, 19585–19593.

Rudner J, Jendrossek V, Belka C (2002) New insights in the role of Bcl-2 Bcl-2 and the endoplasmic reticulum. *Apoptosis* **7**, 441–447.

Rutkowski DT, Kaufman RJ (2007) That which does not kill me makes me stronger: adapting to chronic ER stress. *Trends Biochem. Sci.* **32**, 469–476.

Szegezdi E, Logue SE, Gorman AM, Samali A (2006) Mediators of endoplasmic reticulum stress-induced apoptosis. *EMBO Rep.* **7**, 880–885.

Thomenius MJ, Wang NS, Reineks EZ, Wang Z, Distelhorst CW (2003) Bcl-2 on the endoplasmic reticulum regulates Bax activity by binding to BH3-only proteins. *J. Biol. Chem.* **278**, 6243–6250.

Tirosh B, Iwakoshii NN, Glimcher LH, Ploegh HL (2006) Rapid turnover of unspliced Xbp-1 as a factor that modulates the unfolded protein response. *J. Biol. Chem.* **281**, 5852–5860.

Tseng BP, Green KN, Chan JL, Blurton-Jones M, LaFerla FM (2008) Abeta inhibits the proteasome and enhances amyloid and tau accumulation. *Neurobiol. Aging* **29**, 1607–1618.

Urano F, Wang X, Bertolotti A, Zhang Y, Chung P, Harding HP, Ron D (2000) Coupling of stress in the ER to activation of JNK protein kinases by transmembrane protein kinase IRE1. *Science* **287**, 664–666.

Vattem KM, Wek RC (2004) Reinitiation involving upstream ORFs regulates ATF4mRNA translation in mammalian cells. *Proc. Natl Acad. Sci. USA* **101**, 11269–11274.

Yoshida H (2007) ER stress and diseases. *FEBS J.* **274**, 630–658.

Yoshida H, Okada T, Haze K, Yanagi H, Yura T, Negishi M, Mori K (2000) ATF6 activated by proteolysis binds in the presence of NF-Y (CBF) directly to the cis-acting element responsible for the mammalian unfolded protein response. *Mol. Cell. Biol.* **20**, 6755–6767.

Yoshida H, Matsui T, Yamamoto A, Okada T, Mori K (2001) XBP1 mRNA is induced by ATF6 and spliced by IRE1 in response to ER stress to produce a highly active transcription factor. *Cell* **107**, 881–891.

Yoshida H, Oku M, Suzuki M, Mori K (2006) pXBP1(U) encoded in XBP1 pre-mRNA negatively regulates unfolded protein response activator pXBP1(S) in mammalian ER stress response. *J. Cell Biol.* **172**, 565–575.

Yoshida H, Uemura A, Mori K (2009) pXBP1(U), a negative regulator of the unfolded protein response activator pXBP1(S), targets ATF6 but not ATF4 in proteasome-mediated degradation. *Cell Struct. Funct.* **34**, 1–10.

Zinszner H, Kuroda M, Wang X, Batchvarova N, Lightfoot RT, Remotti H, Stevens JL, Ron D (1998) CHOP is implicated in programmed cell death in response to impaired function of the endoplasmic reticulum. *Genes Dev.* **12**, 982–995.